

TPIFM: A Task-Aware Model for Evaluating Perceptual Interaction Fluency in Remote AR Collaboration

Jiarun Song, *Member, IEEE*, Ninghao Wan, Fuzheng Yang, *Member, IEEE*, Weisi Lin, *Fellow, IEEE*

Abstract—Remote Collaborative Augmented Reality (RCAR) enables geographically distributed users to collaborate by integrating virtual and physical environments. However, because RCAR relies on real-time transmission, it is susceptible to delay and stalling impairments under constrained network conditions. Perceptual interaction fluency (PIF), defined as the perceived pace and responsiveness of collaboration, is influenced not only by physical network impairments but also by intrinsic task characteristics. These characteristics can be interpreted as the task-specific just-noticeable difference (JND), i.e., the maximal tolerable temporal responsiveness before PIF degrades. When the average response time (ART), measured as the mean time per operation from receiving collaborator feedback to initiating the next action, falls within the JND, PIF is generally sustained, whereas values exceeding it indicate disruption. Tasks differ in their JNDs, reflecting distinct temporal responsiveness demands and sensitivities to impairments. From the perspective of the Free Energy Principle (FEP), tasks with lower JNDs impose stricter temporal prediction demands, making PIF more vulnerable to impairments, whereas higher JNDs allow greater tolerance. On this basis, we classify RCAR tasks by JND and evaluate their PIF through controlled subjective experiments under delay, stalling, and hybrid conditions. Building on these findings, we propose the Task-Aware Perceptual Interaction Fluency Model (TPIFM). Experimental results show that TPIFM accurately assesses PIF under network impairments, providing guidance for adaptive RCAR design and user experience optimization under network constraints.

Index Terms—Augmented reality, interaction fluency, delay, stalling, collaboration

I. INTRODUCTION

With the advancement of network, augmented reality (AR) technology is gaining the ability to support real-time remote operation and collaboration [1]-[4]. Remote Collaborative AR (RCAR) enables geographically distributed users to jointly perform tasks by seamlessly overlaying virtual information onto the physical world. Specifically, AR supports direct interaction within real environments, enabling intuitive object manipulation and spatial coordination [5], [6]. Users operate in the physical environments, performing space-based

This work was supported in part by the National Natural Science Foundation of China (62171353) (*Corresponding author: Weisi Lin*).

Jiarun Song and Ninghao Wan are with the School of Telecommunications Engineering, Xidian University, Xi'an, 710071, China (e-mail: jrsong@xidian.edu.cn; ninghaow@stu.xidian.edu.cn).

Fuzheng Yang is with the School of Telecommunications Engineering, Xidian University, China, and with the School of Electrical and Computer Engineering, Royal Melbourne Institute of Technology, Melbourne, VIC 3001, Australia (e-mail: fzhyang@mail.xidian.edu.cn).

Weisi Lin is with the College of Computing and Data Science, Nanyang Technological University, Singapore 639798 (e-mail: wslin@ntu.edu.sg).

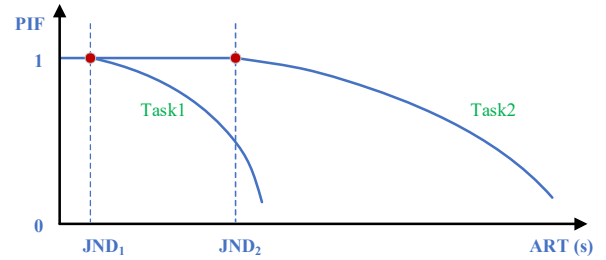


Fig. 1. Illustration of JNDs for two tasks.

actions like hand-based operations and path planning with greater intuitiveness and task adaptability [7]. Moreover, AR is inherently task-oriented, focusing on real-world interaction and operational support through transparent visual feedback and a shared spatial context that enhance decision-making and situational awareness [8]. As a result, RCAR has been widely applied in a variety of practical task-related scenarios such as remote maintenance, collaborative design, training, and medical guidance [9].

RCAR systems primarily support real-time interpersonal collaboration, in which the perceptual interaction fluency (PIF), defined as the subjectively perceived pace and responsiveness of collaboration, is a key dimension of Quality of Experience (QoE) [10], [11]. In RCAR tasks, network impairments such as latency, jitter, and packet loss often cause response delays and stalling [12]-[14], which directly degrade PIF [15]. However, their impact varies across task types, since users' sensitivity and tolerance to impairments depend on the task-specific just-noticeable difference (JND) [16]-[18], defined as the maximal tolerable temporal responsiveness before PIF begins to degrade. As illustrated in Fig. 1, we distinguish two task types. Task1 is a high-tempo, low-cognitive-load turn-taking task, whereas Task2 is a deliberative, turn-based decision-making task. The former requires near-immediate responses, yielding shorter response times and a lower JND (JND_1). When the actual average response time (ART) exceeds JND_1 , users are likely to start to perceive a decline in PIF, making this type more vulnerable to network impairments. The latter involves greater cognitive processing, resulting in longer response times and a higher JND (JND_2), thereby allowing greater tolerance to temporal deviations and more resilient PIF under impairments.

This phenomenon can be explained by the Free Energy Principle (FEP) [19]-[21], which states that the brain minimizes prediction errors (i.e., free energy) by continuously generating predictions of sensory inputs and updating its internal model when discrepancies arise. In RCAR tasks,

> REPLACE THIS LINE WITH YOUR MANUSCRIPT ID NUMBER (DOUBLE-CLICK HERE TO EDIT) <

network-induced delays or stalling impairments disrupt temporal predictions, thereby increasing free energy and prompting cognitive or behavioral adjustments. The extent of this disruption depends on the task-specific JND, where tasks with lower thresholds impose stricter temporal prediction demands, amplifying prediction errors and reducing PIF, whereas tasks with higher thresholds provide greater tolerance and resilience. However, existing research has yet to systematically quantify how these task characteristics influence PIF, highlighting the need to explore their impact for improving system adaptability and enhancing user QoE in RCAR applications.

In this work, to investigate how task-specific JND moderates the impact of delay and stalling on PIF in RCAR scenarios, a series of subjective experiments were conducted on representative RCAR tasks with different JND levels. The effects of latency, stalling, and their combination on PIF across tasks were systematically examined, where delay and stalling were represented by end-to-end (E2E) latency and stalling ratio, respectively. Finally, a Task-Aware Perceptual Interaction Fluency Model (TPIFM) was proposed to evaluate PIF under network impairment in RCAR scenarios. The framework of the proposed model is illustrated in Fig. 2. The main contributions of this work are as follows:

(1) Task-specific JND was introduced as an intrinsic attribute to distinguish RCAR tasks with different temporal responsiveness demands, thereby enabling a task-aware analysis of perceptual interaction fluency (PIF).

(2) Systematic subjective experiments were conducted to examine how JND moderates the effects of delay, stalling, and their combination on PIF, and a task-aware objective evaluation model (TPIFM) was proposed, in which JND is incorporated to effectively quantify PIF under diverse RCAR scenarios.

The rest of this paper is organized as follows: Section II introduces the related work and motivations. Section III presents the experimental design, including the test platform, participants, experimental settings, and procedures. Section IV analyzes the test results and introduces the proposed TPIFM evaluation model. Section V discusses the performance of the model, and Section VI gives the conclusion.

II. RELATED WORK AND MOTIVATIONS

The following section provides a brief overview of the related work and motivation behind this study. Specifically, the related work focuses on the development of RCAR services and the evaluation of QoE in AR-based applications.

A. Development of RCAR Services

In recent years, RCAR services have shown a diversified trend in both technological advancement and application expansion. Currently, RCAR has been widely adopted in key domains like industrial maintenance, emergency management, medical collaboration, and educational innovation [22]-[24]. For example, in industrial maintenance, RCAR systems enable remote experts to provide real-time annotations on equipment

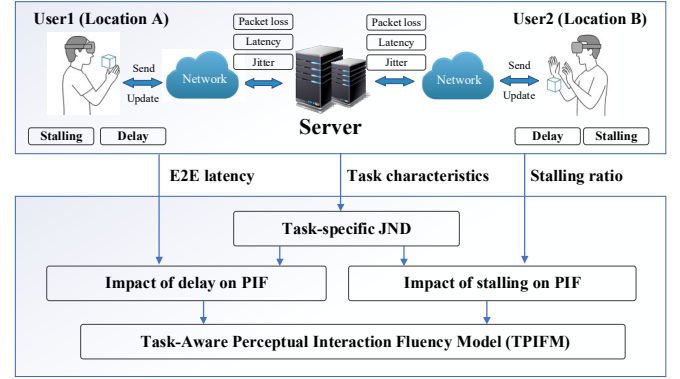


Fig. 2. Framework of perceptual interaction fluency evaluation model.

repair procedures via AR glasses. Virtual instructions are spatially registered and overlaid on the physical surfaces of machinery, allowing on-site technicians to follow these step-by-step guides. This significantly improves operational efficiency and accuracy [4], [22]. In the field of medical collaboration, RCAR technology allows real-time projection of 3D anatomical structures on patients' bodies or surgical areas. Multiple doctors can simultaneously view and interact with shared virtual surgical models using AR devices, supporting remote surgical planning and collaborative procedures with enhanced precision [23]. In educational innovation, RCAR enables the overlay of 3D models (e.g., geological formations or molecular structures) onto laboratory tools or teaching environments. Using AR glasses, teachers and students can engage in immersive knowledge transfer and interactive learning experiences, such as jointly exploring terrain changes, thereby enhancing the intuitive understanding of abstract concepts [24].

To address the diverse characteristics of RCAR services, Sereno et al. [2] proposed a six-dimensional classification framework encompassing time, space, role symmetry, technology symmetry, output devices, and input devices. Time distinguishes between synchronous and asynchronous collaboration, while space refers to whether users are co-located or remote. Role symmetry captures whether users engage in similar or differing roles during collaboration, and technology symmetry assesses whether users employ the same or different hardware setups. The final two dimensions focus on interaction tools, where output devices describe the visual display technologies used (e.g., AR headsets, screens), and input devices refer to interaction methods such as hand tracking, or speech. These dimensions offer a comprehensive framework for analyzing and comparing collaborative AR experiences. Building on this, Marques et al. [7] developed a context-aware classification model, emphasizing the role of semantic understanding in enhancing collaboration effectiveness. Their model systematically characterizes RCAR systems along two key dimensions, namely shared context and dynamic adaptability. Unlike traditional classification methods that primarily address static scenarios, this model provides a theoretical foundation for designing RCAR systems suited to complex and dynamic environments.

> REPLACE THIS LINE WITH YOUR MANUSCRIPT ID NUMBER (DOUBLE-CLICK HERE TO EDIT) <

B. QoE Evaluation of AR-based Services

For RCAR services, delay and stalling are among the most common impairment effects that negatively impact interaction. Although prior studies have tried to reduce the impact of network impairment as much as possible through improvements in interaction algorithms [25]-[27] and optimizations of collaborative network frameworks [28]-[32], these impairments remain difficult to eliminate entirely. Therefore, it is essential to investigate the impact of delay and stalling on QoE in multi-user RCAR scenarios.

In terms of latency-induced impairments, most existing studies have focused on single-user human-computer interactions, using objective metrics like task completion time and error rate [33]-[37]. Recent work has expanded to include user perception, providing latency thresholds across varying contexts. For example, in first-person shooter games, noticeable impairment begins at 75 ms RTT, with severe degradation at 400 ms [38]. In cloud-based social XR, Mitra found that latency within 77 ms has minimal impact on QoE. In mobile AR, users start noticing latency differences at 69 ms, yet show preference for systems below 132 ms, even though performance remains unaffected [39]. For XR tasks such as block-building over video conferencing, acceptable experience is maintained only if E2E latency remains under 900 ms [40]. Meanwhile, AR interaction thresholds vary with task demands, around 75 ms for online gaming and up to 250 ms for telemetry involving the vestibular system [41]. Despite these insights, current approaches remain largely task-specific and fragmented, with reported latency thresholds varying significantly across task types and interaction contexts and lacking unified, systematic evaluation standards. This highlights the need for a more structured latency impact assessment framework that takes into account task urgency and perceptual sensitivity.

Regarding the impact of stalling, existing research primarily focuses on optimizing network performance and designing lightweight E2E AR system architectures [42]-[44]. However, there remains a lack of systematic investigation into how interaction stalling affects user experience quality in multi-user collaborative AR scenarios. For example, [45] highlights that the impact of stalling may vary depending on users' roles within a collaborative task, and that providing clear information about poor network conditions can help mitigate some of the negative effects. The study [46] further explores the differential impact of stalling under task-based and task-free conditions. It finds that users are more sensitive to stalling in non-task situations. This conclusion was not drawn from experiments involving users' active participation in interaction tasks, limiting its generalizability to real-time collaborative contexts. These existing studies largely rely on qualitative methods, such as post-experience questionnaires, and do not offer predictive or computational models of how stalling impairs interaction. Krogfoss et al. [13] proposed a QoE evaluation framework for XR applications over mobile networks that considers the effects of both stalling and delay. This work emphasizes the mapping between Key Quality

Indicators (KQIs) and network-level Key Performance Indicators (KPIs). However, this work does not elaborate on how to design subjective experiments for specific XR scenarios to obtain KPI degradation models. Moreover, it overlooks the influence of multi-user collaboration dynamics and task-dependent variations in QoE perception.

C. Motivations

This paper aims to investigate how task-specific JND modulates the impact of delay and stalling impairments on PIF in RCAR scenarios. The motivation for this work stems from two key considerations:

(1) Compared to traditional 2D video-based collaboration, which relies on indirect input methods such as mouse or touch for limited information exchange, AR enables users to directly perceive, manipulate, and guide task content within the physical environment. This significantly enhances the intuitiveness and efficiency of task execution. In such scenarios, completing real-world tasks requires continuous awareness of the surrounding environment, dynamic feedback processing, and precise manipulation, imposing different and often stricter demands on PIF than conventional 2D interfaces. Therefore, it is essential to conduct dedicated research tailored to AR-based interaction contexts.

(2) The PIF degradation caused by latency and stalling may vary considerably depending on the task-specific JND. Therefore, quantifying how this task characteristic moderates the impact of such impairments on PIF is of importance. For service providers and network operators, understanding task-dependent sensitivity to delay and stalling enables more informed decisions in resource allocation and system optimization. For instance, in tasks with higher JNDs, more complex scene rendering can be applied to enhance immersion, or more concurrent users can be supported without compromising PIF. In contrast, for tasks with lower JNDs, minimizing E2E latency through simplified rendering, efficient transmission schemes, or adaptive designs is critical to maintain smooth interaction.

III. DESIGN OF EXPERIMENTS

To fulfill the objectives of this work, a collaborative task experimental test platform was developed, and a series of subjective experiments were conducted using this platform. Users' subjective ratings of PIF were recorded for model training and verification. The detailed settings of the experiments are presented in the following section.

A. Test platforms

Although RCAR systems have seen preliminary applications in areas such as industrial manufacturing and remote healthcare, the high complexity of interactive tasks, the presence of numerous interfering variables, and the lack of precise control interfaces for delay and stalling impairments make it difficult to ensure that evaluations are conducted under consistent conditions, which limits the quantitative analysis of PIF. To address these challenges, this study develops a multi-user real-time interactive AR test platform,

> REPLACE THIS LINE WITH YOUR MANUSCRIPT ID NUMBER (DOUBLE-CLICK HERE TO EDIT) <

aiming to provide a controllable and repeatable experimental environment. The platform has the following functions: (1) It supports flexible configuration of transmission strategies and realizes dynamic control of E2E latency through frame rendering timing management, (2) It can simulate stalling effects in weak network conditions, and accurately control the frequency and duration of stalling in the interaction process, (3) It integrates an automated rating interface with multi-dimensional data collection capabilities, enabling the synchronous recording of subjective rating scores, user actions, as well as system parameters to support subsequent modeling of PIF. The overall architecture of the platform is shown in Fig 3(a).

Specifically, the virtual object content in the experimental platform is developed based on the Unity3D engine [47] and the Mixed Reality Toolkit (MRTK) [48]. The application is built through the Universal Windows Platform (UWP) and deployed to the Microsoft HoloLens2 devices through Wireless LAN (Wi-Fi). Virtual objects are presented in multiple terminal spaces through a visual sharing mechanism, with data transmission implemented via asynchronous Socket API communication using the TCP protocol [49]. Fig. 3(b) and 3(d) shows the synchronous perspective of remote users moving virtual objects together. The platform allows users to interact with virtual interfaces through hand gestures, which greatly enhances interaction flexibility.

To facilitate analysis and quantitative modeling, the platform enables precise control of impairment parameters. By managing the rendering time of each frame, the system can dynamically regulate the average end-to-end latency. The system's inherent latency is calculated by comparing the network time protocol (NTP) timestamps between the capture time at the sender side and the rendering time at the receiver side. Averaged over 50 independent interaction tests, the inherent system latency is about 15 ms. To dynamically adjust delay of interaction, programmable additional latency is introduced on top of the inherent latency, allowing for fine-grained control and quantitative analysis of E2E latency. To simulate the stalling effects during interactions, the platform extends the rendering duration of specific frames to precisely control the onset and duration of stalling events. During interaction, the system monitors object's pose changes in real time. When stalling conditions are met, it suspends user input responses and freezes the physics engine, resulting in a visual freeze effect. Once the stalling duration ends, system components and physics behaviors automatically resume. This design allows for highly controllable and reproducible simulation of stalling, providing experimental support for studying its impact on PIF.

Additionally, the platform integrates a subjective evaluation interface and automatic data logging. After completing a collaborative task, users are prompted to rate the perceived impact of delay and stalling on PIF, as shown in Fig. 3(c) and Fig. 3(e). All delay and stalling parameters, along with user ratings, are recorded to support the development of evaluation models in AR environments.

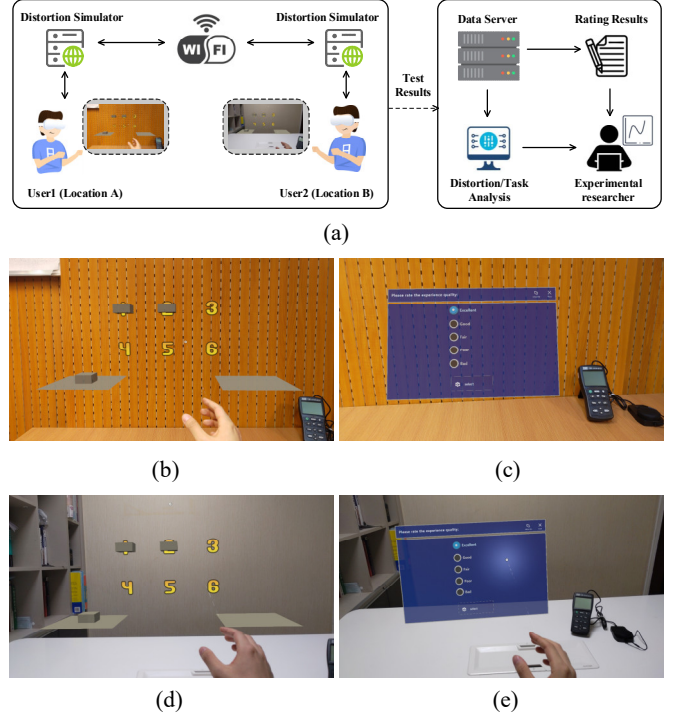


Fig. 3. Illustration of the designed test platform, (a) Architecture of the test platform, (b) User1's perspective, (c) User1's rating interface, (d) User2's perspective, (e) User2's rating interface.

B. Participants

A total of 48 participants aged between 21 and 26 years old ($M=23.5$, $SD=1.2$) were recruited voluntarily for this study, including 20 females (41.6%) and 28 males (58.4%). All were university students and had normal or corrected-to-normal vision and hearing. Six participants (12.5%) reported prior experience with AR devices, while the remaining 42 (87.5%) had no such experience. The study did not collect personal or sensitive data, nor included invasive procedures. The tasks were limited to AR collaboration under controlled laboratory conditions, and thus posed minimal risk to participant. To minimize potential visual fatigue and physical discomfort associated with head-mounted displays, continuous testing in each experiment was restricted to 20 minutes per participant, after which a short break was provided before resuming [50].

C. Experimental settings

The experiment consists of three parts. Experiment1 focuses on task design and JND-based representation. Experiment2 is designed for model training, investigating the effects of delay, stalling, and their combined impact on PIF. Experiment3 is designed to validate the performance of the proposed model.

Experiment 1: Task Design and Representation

Considering that task-specific JND may affect the perception of impairments, it is essential to characterize and quantify this sensitivity for accurate evaluation across different tasks. To this end, six collaborative tasks with varying temporal demands were designed, as illustrated in Fig. 4. The details of each task type are described below.

> REPLACE THIS LINE WITH YOUR MANUSCRIPT ID NUMBER (DOUBLE-CLICK HERE TO EDIT) <

- (1) **Sudoku Puzzle (SP):** Two participants alternately collaborate to complete a 4×4 Sudoku puzzle. Each participant must observe the pattern and spend time thinking before operating, and can only operate after the other participant has completed their turn. This task emphasizes cognitive reasoning rather than rapid action, corresponding to a relatively high JND.
- (2) **Tic-Tac-Toe (TTT):** Two participants alternately place their pieces on a 3×3 grid, aiming to align three pieces in a row, either horizontally, vertically, or diagonally. The first to complete such a line win. This task requires participants to observe the opponent’s move, consider strategies, and decide before placing the next piece. Although the thinking time is short compared with more complex tasks, it still involves reasoning and anticipation of the collaborator’s actions, resulting in slightly slower responses than reflexive tasks.
- (3) **Modular Arithmetic Relay (MAR):** This task is a collaborative activity based on modular arithmetic rules. In each round, a participant receives a random number and performs a modulo operation with a preset divisor. The result determines the placement position of a block (e.g., if $25 \bmod 6$ equals 1, the block is placed in the first position). The task requires participants to calculate quickly and place blocks accurately, with the team aiming to complete an ordered arrangement under specific constraints. By adjusting parameters such as the divisor and number range, the difficulty level can be flexibly modified to promote improvements in both computational efficiency and coordination logic.
- (4) **Block Relay (BR):** This collaborative task involves rapid sequential actions, where participants alternately place 9 blocks in designated positions as quickly as possible. In each round, the system provides a clear target position instruction. Unlike the modular arithmetic domino task, this activity requires no calculations. Participants place the next block immediately after the other completes theirs, continuing until the task is finished. The task emphasizes operational continuity and pace coordination.
- (5) **Laboratory Equipment Sorting (LES):** In this task, two participants collaboratively sort and organize laboratory equipment. One participant is responsible for identifying and selecting the equipment, while the other handles its placement. They take turns operating, and each step must be completed under the partner’s supervision. The next action can only begin once the previous one is finished. This task emphasizes orderly coordination, mutual monitoring, and accurate execution.
- (6) **Vehicle Assembly (VA):** In this task, two participants work together to assemble a virtual vehicle by following a predefined sequence. Each participant takes turns installing different components in the correct positions. A participant must wait until their partner completes the current assembly step before proceeding. This task highlights the importance of stepwise execution and precision in collaborative operations.

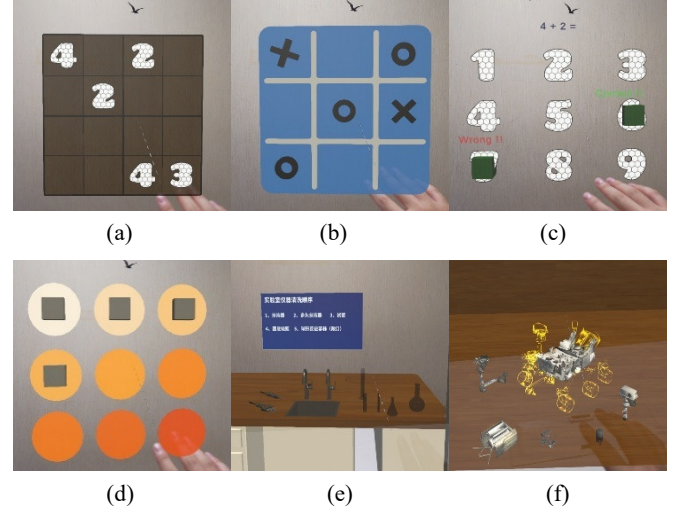


Fig. 4. Task illustration. (a) Sudoku Puzzle (SP), (b) Tic-Tac-Toe (TTT), (c) Modular Arithmetic Relay (MAR), (d) Block Relay (BR), (e) Laboratory Equipment Sorting (LES), (f) Vehicle Assembly (VA).

TABLE I
JND OF EACH TASK

Task	SG	TTT	MAR	BR	LES	VA
JND (s)	3.34	1.57	1.16	0.38	0.71	0.95

To validate the rationality of interactive task settings, a dedicated experiment was conducted with 24 participants. The experiment had two objectives: (1) to assess the effectiveness of task design in differentiating tasks with varying temporal demands, and (2) to measure the JND for each task. These measurements offered empirical support for task classification.

A paired design was used, with participants completing tasks in pairs. The experimental process includes the following operations. In the pilot phase, participants were thoroughly briefed on the experimental procedure and task goals. Each pair was guided into separate experimental environments and assisted by professionals to complete the wearing and calibration of the HoloLens2 headset. For those unfamiliar with AR devices, A five-minute period of free exploration was conducted to help them become acquainted with the device’s operation. After that, participants were given detailed task instructions to ensure smooth execution. In the formal experiment, each pair completed three rounds of all six tasks under ideal network conditions (no delay or stalling). For each task, we computed the baseline average response time (ART_j) under these ideal conditions and used it as a practical proxy for the task’s JND. When the actual ART under impairments (e.g., delay) exceeds ART_j , PIF typically declines.

Table I reports the JND values for each task. A repeated-measures ANOVA showed significant differences across tasks ($F = 547.48, p < .001, \eta^2 = 0.996$), indicating that the task set effectively captures behavioral variation in temporal demand. These results provide a statistically validated basis for distinguishing JND levels across tasks and support the subsequent subjective experiments.

> REPLACE THIS LINE WITH YOUR MANUSCRIPT ID NUMBER (DOUBLE-CLICK HERE TO EDIT) <

Experiment 2: Data Collection for Model Training

This experiment investigates how task-specific JND moderates the impact of delay and stalling on PIF in RCAR scenarios and aims to establish an objective evaluation model. Four task scenarios were tested, including SP, TTT, MAR, and BR. To minimize uncontrolled network interference, all tests were run over a LAN with stable transmission performance. Using reserved interfaces in the test platform, we introduced adjustable delay and stalling via controllable buffering, enabling reliable, level-specific impairment simulation. This setup facilitated a systematic and quantitative analysis of how different network impairments affect PIF, thereby providing empirical evidence to support the construction of an objective evaluation model for PIF under diverse network conditions. Since participants in Experiment 1 had not experienced the testing scenarios of Experiment 2, the same participants were recruited for this study.

Session 1: Experiment on the Impact of Delay

This session takes E2E latency as the research variable of delay effect and designs an experiment under different task scenarios. The experiment sets eight E2E latency levels: 100 ms, 200 ms, 300 ms, 500 ms, 800 ms, 1,000 ms, 2,000 ms, and 3,000 ms. The range spans perceptual thresholds from minimal to severe impairment, ensuring comprehensive coverage of user experience variations. To control for order effects, a Latin square design [51] was adopted to randomize latency levels across multiple groups, thereby improving the reliability and validity of the results.

The experiment consisted of two stages: a pilot study and the formal experiment. In the pilot phase, a stepped delay exposure design was adopted using the BR task as an example. Three levels of latency (100 ms, 800 ms, and 3000 ms) were presented in sequence to establish a baseline for PIF. A five-point Likert scale was constructed in accordance with the ITU-T P.910 Absolute Category Rating (ACR) method [50] to evaluate PIF. The scale consisted of the following levels: "Perfect", "Good", "Fair", "Poor", and "Bad". After each test sequence, participants rated the PIF. The pilot study served to familiarize participants with the task and to help them form an initial understanding of the types of impairment involved.

In the formal experiment, participants completed all tasks in a randomized order. Within each task, they randomly experienced 8 different delay test scenarios. After each test scenario, participants were required to subjectively evaluate the PIF affected by delay. When all the scenarios are evaluated, the current task ended. Participants then removed the HoloLens2 headset and took a five-minute break before proceeding to the next task. This process was repeated until all tasks were completed, marking the end of the experiment. Finally, a total of 768 subjective ratings (8 scenarios \times 4 tasks \times 24 participants) were obtained.

After collecting all subjective ratings from participants in the experiment, the Mean Opinion Scores (MOS) [50] were first calculated to obtain the average perceived rating for each latency configuration per participant. To assess the reliability of experimental data, Pearson Correlation Coefficients (PCC)

TABLE II
PARAMETERS SETTINGS OF STALLING IMPAIRMENT

Index	Times	Duration(ms)	Index	Times	Duration(ms)
1	1	100	8	2	200
2	1	200	9	2	500
3	1	300	10	2	1000
4	1	500	11	3	100
5	1	1000	12	3	200
6	1	2000	13	3	500
7	2	100	14	3	1000

were computed between each participant's individual ratings and the MOS. Participants whose correlation coefficients fell below 0.75 were identified for further examination [50]. For the delay experiment, the average PCC between individual ratings and the corresponding MOS was 0.868, indicating a high level of consistency across participants. Finally, a total of 32 MOS values were obtained through this experiment.

Session 2: Experiment on Impact of Stalling

In this experiment, the effects of stalling on PIF were investigated by manipulating two variables, average stalling duration and stalling frequency, to produce varying levels of impairment across different tasks. The average stalling duration refers to the mean length of each stalling event, while the stalling frequency indicates how often such events occur during an interaction. To ensure the perceptual salience of the impairment, stalling events were triggered within the interaction cycle, specifically 500 milliseconds after the user issued an input command. Each interaction cycle was limited to a single stalling event to avoid overlapping.

The experimental parameters were defined as follows: the average stalling duration in each task was set at six levels, namely 100 ms, 200 ms, 300 ms, 500 ms, 1,000 ms, and 2,000 ms. The stalling frequency was set at 1, 2, or 3 events per task. Using a Latin square design, 14 representative parameter combinations were selected to cover a full range of test conditions from instantaneous mild stalling to long-lasting and severe stalling. The specific stalling parameters for each task are presented in Table II.

Similar to the delay experiment, this test consisted of two phases: a pilot study and a formal experiment. In the pilot phase, a stepped stalling exposure design was employed using the BR task as an example. Three levels of stalling parameters representing perfect to poor interaction conditions were presented to establish a baseline PIF. In the formal experiment, participants completed all tasks in a randomized order. Within each task, they experienced 14 different interaction scenarios, each corresponding to a unique stalling configuration. After completing each scenario, participants provided a subjective rating of PIF based on their perceived stalling effect. Once all scenarios within a task were evaluated, the task was considered complete. Participants then took a standardized five-minute break before proceeding to the next task. This process was repeated until all tasks were completed, marking the end of the experiment. Therefore, a total of 1344 subjective ratings (14 scenarios \times 4 tasks \times 24 participants)

> REPLACE THIS LINE WITH YOUR MANUSCRIPT ID NUMBER (DOUBLE-CLICK HERE TO EDIT) <

were obtained. Following the data processing method used in Session 1, the PCC was calculated for each participant to assess the consistency between individual subjective ratings and the MOS. Finally, the average PCC for the remaining participants in the stalling experiment was 0.878. Finally, a total of 56 MOS values were obtained through this experiment.

Session 3: Experiment on Impact of Combination Effects

This experiment aimed to investigate the impact of combined delay and stalling impairments on PIF in RCAR scenarios. Participants were asked to complete the same set of collaborative tasks as in the previous experiments, where both types of impairment occurred concurrently. The delay and stalling parameters were defined as shown in Table III. For each task, participants experienced 8 test scenarios, each with a unique combination of delay and stalling levels.

The experimental procedure was consistent with that of the previous sessions. During the pilot phase, participants experienced three example trials to familiarize themselves with the experiment procedures. In the formal test, participants completed 8 randomized scenarios for each task. After each scenario, they rated PIF values using a five-point Likert scale, capturing the combined effects of delay and stalling. A total of 768 subjective ratings (8 scenarios \times 4 tasks \times 24 participants) were obtained and corresponding environmental parameters were recorded in parallel. To assess data reliability, PCC were calculated between individual ratings and the MOS. The average PCC across all participants was 0.864. Finally, a total of 32 MOS values were obtained through this experiment.

Experiment 3: Data Collection for Validation

To evaluate the performance of the proposed evaluation model, an additional test was conducted with 24 new participants who had not taken part in any of the previous experiments. In addition to the original TTT and BR tasks, two more application-oriented tasks were introduced, namely, a LES task and a VA task, both designed to better reflect realistic RCAR scenarios. All test scenarios included both delay and stalling impairments, with parameter settings different from those used in Session 3 of Experiment 2. The specific configurations are listed in Table IV. The experimental procedure followed the same protocol as previous sessions. Participants provided subjective ratings of PIF under each condition to validate the performance of the proposed evaluation model. The average PCC across all participants was 0.853. In total, 40 MOS values were collected.

IV. EXPERIMENTAL RESULTS FOR MODELING

This section first analyzes how task-specific JND moderates the impact of delay and stalling impairments on PIF in RCAR scenarios, and then presents a task-aware objective evaluation model that incorporates JND to effectively evaluate PIF.

A. Task-based Modulation of Delay Impacts

Before analyzing the impact of delay on PIF under different tasks, we first conducted the Shapiro-Wilk test [52] to verify whether the participants' scores followed a normal distribution.

TABLE III
PARAMETERS SETTINGS OF DELAY AND STALLING IMPAIRMENT

Index	Delay (ms)	Times of stalling	Avg stalling duration (ms)
1	1000	1	300
2	500	1	1000
3	2000	1	2000
4	800	2	500
5	1000	2	1000
6	2000	2	1000
7	300	3	500
8	2000	3	1000

TABLE IV
CONDITION SETTINGS FOR VALIDATION

Index	Delay (ms)	Times of stalling	Avg stalling duration (ms)
1	200	1	200
2	2000	1	500
3	800	1	1000
4	500	1	2000
5	800	2	300
6	1000	2	400
7	400	2	800
8	200	3	200
9	600	3	400
10	1000	3	1000

The results indicated that the assumption of normality was satisfied for all four tasks: SP ($p = 0.255$), TTT ($p = 0.308$), MAR ($p = 0.446$), and BR ($p = 0.610$). As all p -values were greater than 0.05, the data were deemed appropriate for parametric analysis. A repeated-measures ANOVA was then performed to assess differences between tasks. The test revealed statistically significant variations in MOS values across tasks ($p < 0.05$), demonstrating that the effect of delay on PIF differed significantly depending on the tasks.

Fig. 5 illustrates the trend of PIF (in terms of MOS) as delay (denoted by E2E latency) increases under different tasks. In the SP scenario, MOS scores remained consistently above 3.8 as long as the latency did not exceed 3 seconds, indicating that delay had a minimal impact on PIF. For the TTT task, MOS values stayed above 4 when latency was within 1,000 ms and remained above 3 under delays shorter than 3,000 ms. Overall, as latency increased from 100 ms to 3,000 ms, the MOS decreased gradually in a non-linear manner from 4.6 to 3, reflecting a relatively modest drop of approximately 1.6 points. For the MAR task, MOS maintained above 4 when latency was below 450 ms, and the 3-point threshold was reached at around 1,200 ms. Over the full latency range (100 ms to 3,000 ms), the MOS dropped significantly from 4.7 to 1.8, with a total decline of nearly 3 points. The BR task showed the highest sensitivity to latency. MOS stayed above 4 when latency was below 400 ms, while the 3-point threshold occurred between 600 and 800 ms. When latency exceeded 2,000 ms, the MOS fell to 2. Overall, the MOS plummeted from 4.7 to 1.4 as latency increased from 100 ms to 3,000 ms,

> REPLACE THIS LINE WITH YOUR MANUSCRIPT ID NUMBER (DOUBLE-CLICK HERE TO EDIT) <

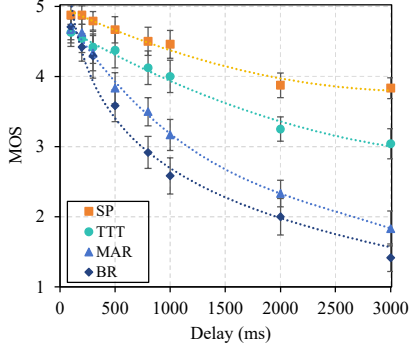


Fig. 5 Relationship between delay and PIF.

marking a drop of over 3 points. Notably, the steepest decline occurred within the 100-800 ms range, after which the degradation trend became more gradual.

The differences in delay sensitivity across tasks are partially attributable to how users cognitively perceive and interpret delays. For example, in the TTT task, participants may introduce substantial subjective delays between interactions due to ongoing cognitive activities such as predicting the opponent's intentions, and formulating a move strategy. These delays are inherently non-deterministic, as participants cannot precisely anticipate the opponent's response timing after making a move. This uncertainty leads to greater variability in delay and raises users' tolerance thresholds, thereby reducing their sensitivity to variations in system-induced delay. In contrast, the BR task requires participants to take turns as quickly as possible, with each participant initiating their move immediately after the partner completes their actions. The absence of deliberate cognitive delay in this task lead to a shorter average response time. Consequently, a heightened sensitivity to even minor delay impairments.

Based on the subjective experimental data presented in Fig. 5, the correlation between PIF and delay was analyzed. The results indicate that PIF follows a negative exponential decay trend as delay increases. Using the least-squares fitting method, we established an objective evaluation model to quantify the relationship between delay and PIF, as expressed below:

$$Q_d = \max(\min(v_1 \cdot \exp(-v_2 \cdot T), 5), 1) \quad (1)$$

where Q_d represents the PIF affected by delay, T_d denotes the E2E latency. v_1 and v_2 are parameters fitted by MATLAB. The parameters for each task are listed in the Table V.

As shown in Table V, parameter v_1 remains constant with increasing JND, therefore, v_1 can be approximately equal to the mean of each task, which equal to 4.751. In contrast, v_2 gradually decreases as JND increases. The relationships between the average response time and parameters v_1 , and v_3 can be expressed as follows:

$$v_2 = \alpha \cdot \exp(-\beta \cdot JND) \quad (2)$$

where $\alpha=6.43e-04$ and $\beta=0.679$ controls the variation trend of v_2 with respect to JND. These parameters are obtained by the least squares fitting using MATLAB.

TABLE V
PARAMETERS OF v_1 AND v_2

Task	JND(s)	v_1	v_2	R -square	RMSE
SP	3.34	4.786	7.99e-05	0.892	0.142
TTT	1.57	4.678	1.56e-04	0.981	0.089
MAR	1.16	4.777	3.57e-04	0.982	0.153
BR	0.38	4.764	4.86e-04	0.956	0.273

B. Task-based Modulation of Stalling Impacts

Before analyzing the impact of stalling impairment on PIF for different tasks, a Shapiro-Wilk test was conducted to assess whether the participant scores in each task followed a normal distribution. The results confirmed normality for all tasks (all p-values > 0.05). Based on this, a repeated-measures ANOVA was performed to examine whether significant differences existed between tasks. The analysis revealed statistically significant variations in MOS scores across tasks ($p < 0.05$), indicating that the impact of stalling on PIF differed significantly depending on the task sceneries.

To facilitate the analysis of stalling impairment, this study uses the parameter stalling ratio R_s to represent different levels of stalling impairment. This ratio is defined as:

$$R_s = \frac{T_s}{T_s + T_m} = \frac{n \cdot T_a}{n \cdot T_a + T_m} \quad (3)$$

where T_s denotes the total duration of stalling events during the task, T_m represents the total duration of user interaction actions, and T_a indicates the average duration of a single stalling event, and n is the number of stalling events.

Fig. 6 presents the PIF (in terms of MOS values) under different stalling ratios for each task. The results indicate that for the same level of stalling (same stalling ratio), the decrease in MOS is relatively small in the SP task, indicating a higher tolerance to stalling impairment. In contrast, in the TTT and MAR tasks, the MOS drops more noticeably, reflecting a stronger impact of stalling on PIF. The BR task shows the steepest decline, where MOS values decrease rapidly as the R_s increases, indicating that PIF is highly sensitive to stalling in this task.

This result aligns with expectations, indicating that task-specific JNDs play a key role in shaping PIF. In tasks with low JNDs, such as BR, interactions occur in rapid succession, and participants often form an expected pace. In such cases, a stalling event can interrupt this pace and affect subsequent actions, amplifying the perceived disruption. By contrast, in tasks with high JNDs, such as SP and TTT, longer intervals between interactions allow more time for cognitive processing, reducing users' sensitivity to brief disruptions and thereby lessening the impact of stalling on PIF.

Based on the subjective evaluation results from the stalling experiment, the PIF decreases with R_s following a negative exponential trend. Using the least squares method, the relationship can be expressed as follows:

$$Q_s = \max(\min(v_3 \cdot \exp(-v_4 \cdot R_s), 5), 1) \quad (4)$$

> REPLACE THIS LINE WITH YOUR MANUSCRIPT ID NUMBER (DOUBLE-CLICK HERE TO EDIT) <

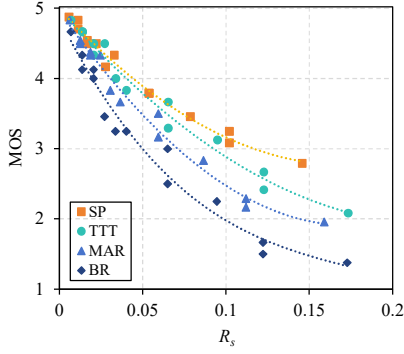


Fig. 6. Relationship between R_s and PIF.

TABLE VI
PARAMETERS OF v_3 AND v_4

Task	JND(s)	v_3	v_4	<i>R-square</i>	<i>RMSE</i>
SP	3.34	4.905	4.282	0.976	0.110
TTT	1.57	4.965	5.301	0.976	0.145
MAR	1.16	4.911	6.611	0.978	0.147
BR	0.38	4.937	9.291	0.956	0.230

where Q_s represents the PIF under stalling conditions, while R_s denotes the stalling ratio. Parameters v_3 and v_4 were fitted through MATLAB, as shown in Table VI. The parameter v_3 is related to the maximum value of MOS. It can be seen that the maximum values of different tasks are relatively close, and the v_3 value also remains relatively stable, close to a constant value of about 4.929. In contrast, v_4 is related to the curvature, and it exhibits noticeable variation under different tasks.

As shown in Table VI, parameter v_4 gradually decreases as the JND increases. The relationship between v_4 and the JND can be expressed as follows:

$$v_4 = \rho \cdot JND^{-\sigma} \quad (5)$$

where, $\rho=6.608$, and $\sigma=0.361$ mainly control the variation trend of v_4 with JND. These parameters are obtained by least squares fitting using MATLAB.

C. PIF evaluation model

In this section, an PIF evaluation model was proposed for different RCAR tasks combining the impact of both delay and stalling effects. Considering both delay and stalling have negative impacts on PIF, the PIF under the combined influence of delay and stalling can be expressed as follows:

$$Q = \max\left(\min\left(4 \times (1 - v_5 \cdot (5 - Q_d)) - v_6 \cdot (5 - Q_s)\right) + 1, 5\right), 1) \quad (6)$$

where Q is the PIF that affected by delay and stalling effect. $v_5=0.104$ and $v_6=0.192$ are weight values which are obtained by the least square fitting method using the data of Session 3 of Experiment 2. According to the fitting results, the impact of stalling seems slightly greater than that of delay on the PIF.

In summary, this study focuses on RCAR applications and incorporates task-dependent characteristics to analyze the effects of delay, stalling, and their combined impact on PIF

across different tasks. Based on these analyses, a comprehensive evaluation model for PIF was developed. This model is applicable to realistic RCAR task scenarios where both delay and stalling effects may be present.

V. PERFORMANCE EVALUATION

To validate the performance of the proposed model, the results obtained from Experiment 3 were employed in this section. For comparison, three baseline models that do not account for task-specific characteristics were selected (referred to as Baseline1, Baseline2, and Baseline3). Specifically, Baseline1 model adopts the same structure as the proposed model in Eq (6), where Q_d and Q_s are predicted using Eqs (1) and (4), respectively. However, the parameters are fitted using aggregated data from all four tasks without distinguishing between task types. The fitted parameters are: $v_1=4.726$, $v_2=0.0002$, $v_3=4.878$, $v_4=6.096$. Baseline2 follows the dual-exponential form proposed in [13] and is defined as:

$$Q_{baseline2} = \max\left(\min\left(4 \times a \cdot \exp(b \cdot T) \times \exp\left(-\frac{SR}{s}\right) + 1, 5\right), 1\right) \quad (7)$$

where T denotes the delay and SR represents the stalling ratio. The fitted parameters are $a=1.07$, $b=-0.24$, and $s=0.15$. Among them, a and b adjust the influence of delay, while s adjusts the influence of stalling. Baseline3 adopts a linear formulation referenced from [14], which is defined as:

$$Q_{baseline3} = \max\left(\min(l_0 + l_1 \cdot T + l_2 \cdot SR, 5), 1\right) \quad (8)$$

where l_1 and l_2 indicates the weight of the delay and stalling effects. Specifically, $l_0=4.208$, $l_1=-0.0003$, and $l_2=-12.39$.

Three typical metrics specified by VQEG, namely the PCC, the Spearman Rank Order Correlation Coefficient (SROCC), and the Root Mean Squared Error (RMSE), were employed in the performance validation [53]. Generally, a smaller value of the RMSE and a larger value of the PCC and SROCC values indicate superior performance. Table VII lists the evaluation performance in terms of these metrics under different validation datasets. It can be found that the proposed model achieves higher PCC and SROCC values and a lower RMSE compared to the other baseline models, demonstrating its superior ability to predict PIF across different task scenarios. At the same time, we followed [54] to perform an F-test on the residual between MOS and predicted PIF to check the significance of performance difference between the baseline model and the proposed model. The F-test results show that all p-values (sig.) are less than 0.05, indicating that the evaluation performance of the proposed model is significantly different from that of the baseline model, and the evaluation performance is significantly improved when the proposed model is used.

Fig. 7 provides scatter plots of MOS and the predicted interactive quality to intuitively clarify the performance across different tasks. To evaluate task-dependent prediction accuracy, results are grouped by task type. As shown in Fig. 7,

> REPLACE THIS LINE WITH YOUR MANUSCRIPT ID NUMBER (DOUBLE-CLICK HERE TO EDIT) <

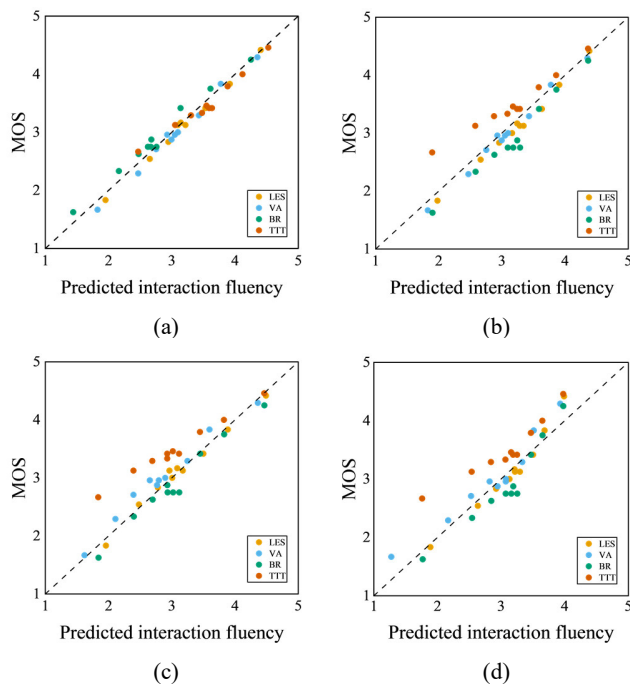


Fig. 7. Scatter plots of predicted PIF and MOS. (a) Proposed model, (b) Baseline1, (c) Baseline2, (d) Baseline3.

TABLE VII
PERFORMANCE OF THE EVALUATION MODEL

Model	Task	PCC	SORCC	RMSE
Baseline1	LES	0.995	0.960	0.145
	VA	0.991	0.960	0.096
	BR	0.985	0.963	0.314
	TTT	0.983	0.960	0.364
Baseline2 [13]	LES	0.993	0.960	0.079
	VA	0.988	0.979	0.184
	BR	0.988	0.914	0.189
	TTT	0.993	0.960	0.492
Baseline3 [14]	LES	0.976	0.960	0.170
	VA	0.966	0.979	0.219
	BR	0.956	0.963	0.288
	TTT	0.948	0.960	0.455
Proposed model (TPIFM)	LES	0.997	0.979	0.089
	VA	0.996	0.979	0.109
	BR	0.994	0.963	0.156
	TTT	0.983	0.960	0.134
	All	0.985	0.986	0.124

the proposed model consistently delivers accurate predictions under all tasks, with predicted scores closely aligning with subjective user ratings. This indicates that the proposed model effectively captures task-dependent characteristics and maintains robust predictive capability across varying interaction tasks. In contrast, the baseline models show varying levels of performance across tasks. Specifically, while they perform relatively well in tasks with moderate task-specific JNDs, such as VA and LES, their accuracy drops noticeably in tasks with low JNDs, such as BR. These results

suggest that baseline models lack the adaptability to task-specific characteristics and are more prone to performance inconsistencies under varying temporal demands.

VI. CONCLUSION

This study investigates how task-specific JNDs moderate the impact of delay and stalling on PIF through a series of controlled subjective experiments. The findings demonstrate that both E2E latency and stalling have negative effects on PIF. However, in tasks with low JNDs, where users have stronger temporal expectations regarding responsiveness, these impairments are perceived as more disruptive. In contrast, users performing tasks with high JNDs exhibit greater tolerance to variations in delay and stalling due to weaker reliance on precise temporal coordination. From the perspective of FEP, this asymmetry arises because tasks with lower JNDs impose stricter temporal prediction demands, whereas higher JNDs allow greater flexibility in minimizing prediction errors. Based on these insights, a task-aware objective evaluation model (TPIFM) is proposed, which incorporates task-specific JND to assess PIF under delay and stalling conditions in RCAR scenarios. Experimental validation confirms that TPIFM achieves higher prediction accuracy than models that ignore task characteristics, providing both theoretical support for FEP-based interpretations of task sensitivity and practical guidance for adaptive optimization in RCAR systems.

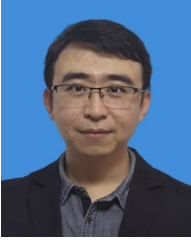
REFERENCES

- [1] G. Pan, S. Xu, S. Zhang, et al. "Quality of experience oriented cross-layer optimization for real-time XR video transmission," *IEEE Transactions on Circuits and Systems for Video Technology*, vol. 34, no. 8, pp. 7742-7755, 2024.
- [2] M. Sereno, X. Wang, L. Besançon, et al. "Collaborative work in augmented reality: A survey," *IEEE Transactions on Visualization and Computer Graphics*, vol. 28, no. 6, pp. 2530-2549, 2020.
- [3] A. Schäfer, G. Reis, D. Stricker. "A survey on synchronous augmented, virtual, and mixed reality remote collaboration systems," *ACM Computing Surveys*, vol. 55, no. 6, pp. 1-27, 2022.
- [4] D. Fang, H. Xu, X. Yang, et al. "An augmented reality-based method for remote collaborative real-time assistance: from a system perspective," *Mobile Networks and Applications*, vol. 25, pp. 412-425, 2020.
- [5] F. Tang, Y. Wu, X. Hou, et al. "3D mapping and 6D pose computation for real time augmented reality on cylindrical objects," *IEEE Transactions on Circuits and Systems for Video Technology*, vol. 30, no. 9, pp. 2887-2899, 2019.
- [6] X. Zhang, X. Bai, S. Zhang, et al. "Real-time 3D video-based MR remote collaboration using gesture cues and virtual replicas," *The International Journal of Advanced Manufacturing Technology*, vol. 121, no. 11, pp. 7697-7719, 2022.
- [7] B. Marques, S. Silva, J. Alves, et al. "A conceptual model and taxonomy for collaborative augmented reality," *IEEE Transactions on Visualization and Computer Graphics*, vol. 28, no. 12, pp. 5113-5133, 2021.
- [8] J. Fu, A. Rota, S. Li, et al. "Recent advancements in augmented reality for robotic applications: A survey," *Actuators*, MDPI, vol. 12, no. 323, pp.1-29, 2023.
- [9] P. Wang, X. Bai, M. Billingham, et al. "AR/MR remote collaboration on physical tasks: a review," *Robotics and Computer-Integrated Manufacturing*, vol. 72: 102071, pp. 1-32, 2021.
- [10] G. Hoffman, "Evaluating fluency in human-robot collaboration," *IEEE Transactions on Human-Machine Systems*, vol. 49, no. 3, pp. 209-218, 2019.
- [11] S. Egger, P. Reichl, K. Schoenenberg. "Quality of experience and interactivity," *Quality of Experience: Advanced Concepts, Applications and Methods*. Cham: Springer International Publishing, 2014, pp. 149-161.

> REPLACE THIS LINE WITH YOUR MANUSCRIPT ID NUMBER (DOUBLE-CLICK HERE TO EDIT) <

- [12] ITU-T Recommendation G.1036. "Quality of experience influencing factors for augmented reality services," 2022, July.
- [13] B. Krogfoss, J. Duran, P. Perez, et al. "Quantifying the value of 5G and edge cloud on QoE for AR/VR" in *Proc. IEEE Twelfth International Conference on Quality of Multimedia Experience (QoMEX)*, 2020, pp.1-4.
- [14] H. Rossi, K. Mitra, C. Åhlund, et al. "QoE models for virtual reality Cloud-based first person shooter game over mobile networks," in *Proc. 20th IEEE CNSM*, 2024, pp.1-5.
- [15] Y. Huang, L. Cao, H. Zhang, et al. "Model between Network Quality and XR User's Experience in Terms of Video Stalling for Cloud Rendering XR," *IEEE Access*, vol. 13, pp.1-11, 2025.
- [16] W. Lin, G. Ghinea, "Progress and opportunities in modelling just-noticeable difference (JND) for multimedia," *IEEE Transactions on Multimedia*, vol. 24, pp. 3706-3721, 2021.
- [17] J. Jin, X. Zhang, X. Fu, et al. "Just noticeable difference for deep machine vision," *IEEE Transactions on Circuits and Systems for Video Technology*, vol. 32, no. 6, pp. 3452-3461, 2021.
- [18] Q. Jiang, F. Liu, Z. Wang, et al. "Rethinking and conceptualizing just noticeable difference estimation by residual learning," *IEEE Transactions on Circuits and Systems for Video Technology*, vol. 34, no. 10, pp. 9515-9527, 2024.
- [19] K. Friston. "The free-energy principle: a unified brain theory?" *Nature Reviews Neuroscience*, vol.11, no. 2, pp. 127-138, 2010.
- [20] K. Gu, W. Lin, G. Zhai, et al. "No-reference quality metric of contrast-distorted images based on information maximization." *IEEE Transactions on Cybernetics*, vol. 47, no. 12, pp. 4559-4565, 2016.
- [21] Y. Zhang, S. Zhang, N. Li, et al. "VP-JND: Visual Perception Assisted Deep Picture-Wise Just Noticeable Difference Prediction Model for Image Compression," *IEEE Transactions on Circuits and Systems for Video Technology*, 2025 (Early Access).
- [22] R. Palmirani, J. A. Erkoyuncu, R. Roy, et al. "A systematic review of augmented reality applications in maintenance," *Robotics and Computer-Integrated Manufacturing*, vol. 49, pp. 215-228, 2018.
- [23] K. Yu, U. Eck, F. Pankratz, et al. "Duplicated reality for co-located augmented reality collaboration," *IEEE Transactions on Visualization and Computer Graphics*, vol. 28, no. 5, pp. 2190-2200, 2022.
- [24] S. Lu, Y. Lin, K. Tan, et al. "Revolutionizing elementary disaster prevention education and training via augmented reality-enhanced collaborative learning," *International Journal of Engineering Business Management*, vol. 14: 18479790211067345, 2022.
- [25] W. He, B. Swift, H. Gardner, et al. "Reducing latency in a collaborative augmented reality service," in *Proc. 17th International Conference on Virtual-Reality Continuum and its Applications in Industry*. 2019, pp.1-9.
- [26] Y. Choi, W. Son, Y. S. Kim. "A Study on Interaction Prediction for Reducing Interaction Latency in Remote Mixed Reality Collaboration," *Applied Sciences*, vol. 11, no. 22, pp. 1-18, 2021.
- [27] W. Zhang, B. Han, P. Hui, et al. "CARS: Collaborative augmented reality for socialization," in *Proc. 19th International Workshop on Mobile Computing Systems & Applications*. 2018, pp. 25-30.
- [28] P. Ren, X. Qiao, Y. Huang, et al. "Edge AR X5: An edge-assisted multi-user collaborative framework for mobile web augmented reality in 5G and beyond," *IEEE Transactions on Cloud Computing*, vol. 10, no. 4, pp. 2521-2537, 2020.
- [29] Y. Siriwardhana, P. Porambage, M. Liyanage, et al. "A survey on mobile augmented reality with 5G mobile edge computing: Architectures, applications, and technical aspects," *IEEE Communications Surveys & Tutorials*, vol. 23, no. 2, pp. 1160-1192, 2021.
- [30] C. Durugbo. "Collaborative networks: a systematic review and multi-level framework," *International Journal of Production Research*, vol. 54, no. 12, pp. 3749-3776, 2016.
- [31] D. G. Morín, P. Pérez, A. G. Armada. "Toward the distributed implementation of immersive augmented reality architectures on 5G networks," *IEEE Communications Magazine*, vol. 60, no. 2, pp. 46-52, 2022.
- [32] M. Torres Vega, C. Liaskos, S. Abadal, et al. "Immersive interconnected virtual and augmented reality: A 5G and IoT perspective," *Journal of Network and System Management*, vol. 28, pp. 796-826, 2020.
- [33] M. Nabiyouni, S. Scerbo, D. A. Bowman, and T. Hollerer, "Relative effects of real-world and virtual-world latency on an augmented reality training task: an AR simulation experiment," *Frontiers in ICT*, vol. 3, pp. 1-13, 2017.
- [34] T. Khan, T. Zhu, T. Downes, et al. "Understanding effects of visual feedback delay in AR on fine motor surgical tasks," *IEEE Transactions on Visualization and Computer Graphics*, vol. 29, no.11, pp. 4697-4707, 2023.
- [35] C. Lee, S. Bonebrake, D. A. Bowman, et al. "The role of latency in the validity of AR simulation," in *Proc. 2010 IEEE Virtual Reality Conference (VR)*. IEEE, 2010, pp. 11-18.
- [36] P. Caserman, M. Martinussen, S. Göbel. "Effects of end-to-end latency on user experience and performance in immersive virtual reality applications," in *Proc. Joint International Conference on Entertainment Computing and Serious Games*. Cham: Springer International Publishing, 2019, pp. 57-69.
- [37] T. Waltemate, I. Senna, F. Hülsmann, et al. "The impact of latency on perceptual judgments and motor performance in closed-loop interaction in virtual reality," in *Proc. 22nd ACM Conference on Virtual Reality Software and Technology*. 2016, pp. 27-35.
- [38] H. S. Rossi, K. Mitra, S. Larsson, et al. "Subjective qoe assessment for virtual reality cloud-based first-person shooter game," in *Proc. ICC 2024-IEEE International Conference on Communications*. IEEE, 2024, pp. 4698-4703.
- [39] K. Mitra, H. S. Rossi, J. Gavrell, et al. "QoE assessment of cloud-based social extended reality applications over heterogeneous access networks," in *Proc. 2025 IEEE 22nd Consumer Communications & Networking Conference (CCNC)*. IEEE, 2025, pp. 1-2.
- [40] C. Cortés, I. Viola, J. Gutiérrez, et al. "Delay threshold for social interaction in volumetric eXtended Reality communication," *ACM Transactions on Multimedia Computing, Communications and Applications*, vol. 20, no. 7, pp. 1-22, 2024.
- [41] X. Shen, J. Gao, M. Li, et al. "Toward immersive communications in 6G," *Frontiers in Computer Science*, 2023, vol. 4: 1068478, pp. 1-31.
- [42] Y. Siriwardhana, P. Porambage, M. Liyanage, et al. "A survey on mobile augmented reality with 5G mobile edge computing: Architectures, applications, and technical aspects," *IEEE Communications Surveys & Tutorials*, vol. 23, no. 2, pp. 1160-1192, 2021.
- [43] D. G. Morín, P. Pérez, A. G. Armada. "Toward the distributed implementation of immersive augmented reality architectures on 5G networks," *IEEE Communications Magazine*, vol. 60, no. 2, pp. 46-52, 2022.
- [44] Y. Wen, A. B. Shah, R. Cao, et al. "AR-Light: enabling fast and lightweight multi-user augmented reality via semantic segmentation and collaborative view synchronization," *IEEE Transactions on Computers*, vol.71, no. 6, pp. 2073-2086, 2025.
- [45] T. Ahsen, Z. Lim, A. Gardony, et al. "The effects of network outages on user experience in augmented reality based remote collaboration - an empirical study," in *Proc. ACM on Human-Computer Interaction*, pp. 1-27, 2021.
- [46] T. M. C. Chu, M. Fiedler, V. Kelkkanen, et al. "On the perception of frame stalls in remote VR for task and task-free subjective tests," in *Proc. 15th International Conference on Quality of Multimedia Experience (QoMEX)*. IEEE, 2023, pp. 201-204.
- [47] J. Xie. "Research on key technologies base Unity3D game engine," in *Proc. 2012 7th international conference on computer science & education (ICCSE)*. IEEE, 2012, pp. 695-699.
- [48] A. Caputo, R. Bartolomioli, A. Giachetti. "Remote and deviceless manipulation of virtual objects in mixed reality," in *Proc. Smart tools and Applications in Graphics-Eurographics Italian Chapter Conference*. 2023, pp. 1-11.
- [49] Y. Tian, K. Xu, N. Ansari. "TCP in wireless environments: problems and solutions," *IEEE Communications Magazine*, vol. 43, no. 3, pp. S27-S32, 2005.
- [50] ITU-T Recommendation P.910. "Methods for the subjective assessment of video quality, audio quality and audiovisual quality of Internet video and distribution quality television in any environment," 2023.
- [51] B. G. Kim, H. H. Stein. "A spreadsheet program for making a balanced Latin square design," *Revista Colombiana de Ciencias Pecuaris*, vol. 22, no. 4, pp. 591-596, 2009.
- [52] Z. Hanusz, J. Tarasinska, W. Zielinski. "Shapiro-Wilk test with known mean," *REVSTAT-statistical Journal*, vol. 14, no. 1, pp. 89-100, 2016.
- [53] Final report from the video quality experts group on the validation of objective models of video quality assessment, Phase II 2003 Video Quality, Experts Group (VQEG).
- [54] K. Seshadrinathan, R. Soundararajan, A. C. Bovik, and L. K. Cormack, "Study of subjective and objective quality assessment of video," *IEEE Transactions on Image Processing*, vol. 19, no. 6, pp. 1427-1441, 2010.

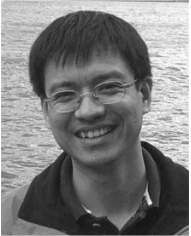
> REPLACE THIS LINE WITH YOUR MANUSCRIPT ID NUMBER (DOUBLE-CLICK HERE TO EDIT) <



Jiarun Song (Member, IEEE) received the B.S. and Ph.D. degrees from Xidian University, Xi'an, China in 2009 and 2015, respectively. He is currently an Associate Professor with the State Key Laboratory of Integrated Services Networks, Xidian University. His research interests focus on QoE, video quality assessment, and multimedia communication.

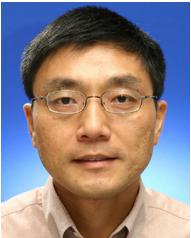


Ninghao Wan received the B.S. degree in Telecommunication Engineering from Xidian University, Xi'an, China, in 2024. He is currently a graduate student in the Xidian University. His research interests include Virtual/Augmented Reality, video quality assessment, and multimedia communication.



Fuzheng Yang (Member, IEEE) received the B.E. degree in Telecommunication Engineering, the M.E. degree and the Ph.D. in Communication and Information System from Xidian University, Xi'an, China, in 2000, 2003 and 2005, respectively. He became a lecturer and an Associate Professor in Xidian University in 2005 and 2006, respectively. He has been a professor of communications engineering with Xidian University since 2012.

He is also an Adjunct Professor of School of Engineering in RMIT University. During 2006-2007, he served as a visiting scholar and postdoctoral researcher in Department of Electronic Engineering in Queen Mary, University of London. His research interests include video quality assessment, video coding and multimedia communication.



Weisi Lin (Fellow, IEEE) received the Ph.D. degree from the King's College, University of London, U.K. He is currently a Professor with the College of Computing and Data Science, Nanyang Technological University. His areas of expertise include image processing, perceptual signal modeling, video compression, and multimedia communication, in which he has published over 200 journal articles, over 230 conference papers, filed seven patents, and authored two books. He has been an invited/panelist/keynote/tutorial speaker at over 20 international conferences. He is a fellow of IET and an Honorary Fellow of Singapore Institute of Engineering Technologists. He has been the Technical Program Chair of IEEE ICME 2013, PCM 2012, QoMEX 2014, and IEEE VCIP 2017. He has been an Associate Editor of IEEE TRANSACTIONS ON IMAGE PROCESSING, IEEE TRANSACTIONS ON CIRCUITS AND SYSTEMS FOR VIDEO TECHNOLOGY, IEEE TRANSACTIONS ON MULTIMEDIA, and IEEE SIGNAL PROCESSING LETTERS. He was a Distinguished Lecturer of Asia-Pacific Signal and Information Processing Association (APSIPA) from 2012 to 2013 and the IEEE Circuits and Systems Society from 2016 to 2017.